

The Yeast Homolog of Heme Oxygenase-1 Affords Cellular Antioxidant Protection via the Transcriptional Regulation of Known Antioxidant Genes^{*[5]}

Received for publication, September 28, 2010, and in revised form, November 10, 2010. Published, JBC Papers in Press, November 16, 2010, DOI 10.1074/jbc.M110.187062

Emma J. Collinson[‡], Sabine Wimmer-Kleikamp^{‡1}, Sebastien K. Gerega[§], Yee Hwa Yang[¶], Christopher R. Parish^{||}, Ian W. Dawes^{**}, and Roland Stocker^{‡2}

From the [‡]Centre for Vascular Research, School of Medical Sciences (Pathology) and Bosch Institute, Sydney Medical School, [§]Sydney Bioinformatics, and the [¶]School of Mathematics and Statistics, University of Sydney, Sydney, New South Wales 2006, Australia, the ^{||}John Curtin School of Medical Research, The Australian National University, Canberra, Australian Capital Territory 2601 Australia, and the ^{**}Ramaciotti Centre for Gene Function Analysis, School of Biotechnology and Biomolecular Science, University of New South Wales, Sydney, New South Wales 2052, Australia

Heme oxygenase-1 (HO-1) degrades heme and protects cells from oxidative challenge. This antioxidant activity is thought to result from the HO-1 enzymatic activity, manifested by a decrease in the concentration of the pro-oxidant substrate heme, and an increase in the antioxidant product bilirubin. Using a global transcriptional approach, and yeast as a model, we show that HO-1 affords cellular protection via up-regulation of transcripts encoding enzymes involved in cellular antioxidant defense, rather than via its oxygenase activity. Like mammalian cells, yeast responds to oxidative stress by expressing its HO-1 homolog and, compared with the wild type, heme oxygenase-null mutant cells have increased sensitivity toward oxidants that is rescued by overexpression of human HO-1 or its yeast homolog. Increased oxidant sensitivity of heme oxygenase-null mutant cells is explained by a decrease in the expression of the genes encoding γ -glutamylcysteine synthetase, glutathione peroxidase, catalase, and methionine sulfoxide reductase, because overexpression of any of these genes affords partial, and overexpression of all four genes provides complete, protection to the null mutant. Genes encoding antioxidant enzymes represent only a small portion of the 480 differentially expressed transcripts in heme oxygenase-null mutants. Transcriptional regulation may be explained by the nuclear localization of heme oxygenase observed in oxidant-challenged cells. Our results challenge the notion that HO-1 functions simply as a catabolic and antioxidant enzyme. They indicate much broader functions for HO-1, the unraveling of which may help explain the multiple biological responses reported in animals as a result of altered HO-1 expression.

Heme oxygenase degrades heme to CO, Fe²⁺, and biliverdin (1). Mammalian cells contain heme oxygenase-1 (HO-1)³ and HO-2 that share 43% amino acid sequence homology (2). Compared with HO-2, HO-1 has a lower apparent K_m -value for heme (3), and the two enzymes are regulated differently and exhibit different physiological properties (4). The constitutively expressed HO-2 is implicated in oxygen sensing (5) and contains heme regulatory motifs that act as a thiol/disulfide redox switch, regulating the K_d for ferric heme (6). In most tissues HO-1 expression is induced in response to different types of stress, including oxidative stress, heat shock, and iron starvation (4). Increased expression of HO-1 is associated with a range of different cellular properties, including increased antioxidant protection and altered cell growth and signaling (4). In addition, there is mounting evidence suggesting that induction of HO-1 protects against various diseases (7, 8).

Prokaryotes and lower eukaryotes possess homologs of mammalian HO-1. In the case of *Saccharomyces cerevisiae*, the homolog Hmx1p was identified as a stress protein in response to iron deprivation (9), and in a genome-wide transcriptional investigation of the activator of ferrous transport (*AFT1*) regulon (10). Aft1p is an iron-dependent transcription factor (11) that induces the expression of several genes, including *HMX1*, in response to iron limitation. Several lines of evidence support a role for Hmx1p in the regulation of heme and iron homeostasis in yeast. Deletion of *HMX1* leads to the accumulation of heme and depletion of iron, as well as to the expression of *FET3*, a known Aft1p target gene that encodes a multi-copper oxidase (12) and that forms part of a high affinity iron transport complex (13). Loss of *HMX1* also leads to the induction of *CYCI* via the oxygen-sensing transcription factor Hap1p that itself is activated by heme (14). Heme acts

* This work was supported by the Australian Research Council DP0988470, University of Sydney Medical Foundation, and the National Health & Medical Research Council of Australia (NHMRC) Program Grant 455395.

[5] The on-line version of this article (available at <http://www.jbc.org>) contains supplemental Figs. S1–S5 and Tables S1–S4.

¹ Supported by a NHMRC CJ Martin Fellowship and an Early Career Grant of the Sydney Medical School.

² Supported by a NHMRC Senior Principal Research Fellowship and a University of Sydney Professorial Fellowship. To whom correspondence should be addressed: Centre for Vascular Research, School of Medical Sciences (Pathology) and Bosch Institute, Sydney Medical School, University of Sydney, Sydney, NSW 2006. Tel.: 61-2-9036-3207; Fax: 61-2-9036-3038; E-mail: roland.stocker@sydney.edu.au.

³ The abbreviations used are: HO-1, heme oxygenase-1; *CTT1*, gene encoding cytosolic catalase; *GPX1*, gene encoding a glutathione peroxidase that acts on phospholipid hydroperoxides/non-phospholipid and other organic peroxides; *GPX2*, gene encoding an atypical 2-Cys peroxidoxin; *GSH1*, gene encoding γ -glutamylcysteine synthetase; HA-HMX1p, N-terminus HA-tagged Hmx1p; Hmx1p, yeast heme oxygenase protein; *HMX1*, gene encoding yeast heme oxygenase; HMX1-HAp, C terminus tagged Hmx1p; *MXR1*, gene encoding peptide methionine sulfoxide reductase; H₂O₂, hydrogen peroxide.

TABLE 1

Glutathione content and activities of antioxidant enzymes the genes of which are differently expressed in wild type and *hmx1* mutant strains
Cells transformed with a galactose-inducible multi-copy plasmid containing *HMX1* or *MXR1* were grown to exponential phase in raffinose- (non-induced) or galactose-containing medium (induced), lysed, and total glutathione and antioxidant enzyme activities determined as described under "Experimental Procedures." Results show mean \pm S.E. of three separate experiments.

Strain	Total glutathione	Catalase	GSH peroxidase	Methionine sulfoxide reductase
	$\mu\text{mol}/\text{min}/\text{mgp}$	$\mu\text{mol}/\text{min}/\text{mgp}$	$\mu\text{mol}/\text{min}/\text{mgp}$	$\text{nmol}/\text{min}/\text{mgp}$
wt	1.0 \pm 0.1	87.0 \pm 6.3	13.8 \pm 1.1	ND ^a
wt <i>HMX1</i> non-induced	1.2 \pm 0.1	95.5 \pm 1.8	14.7 \pm 0.4	ND
wt <i>HMX1</i> induced	5.7 \pm 0.4 ^b	368.6 \pm 15.9 ^b	37.2 \pm 3.3 ^b	ND
<i>hmx1</i>	0.2 \pm 0.1 ^b	27.6 \pm 2.4 ^b	12.1 \pm 0.3	ND
<i>hmx1 HMX1</i> non-induced	0.2 \pm 0.1 ^b	29.1 \pm 1.3 ^b	10.1 \pm 0.7 ^b	ND
<i>hmx1 HMX1</i> induced	1.7 \pm 0.1 ^b	214.4 \pm 4.8 ^b	18.4 \pm 1.0	ND
wt <i>MXR1</i> induced	NT ^c	NT	NT	1.3 \pm 0.2

^a ND, not detectable (detection limit, 0.1 nmol/min/mgp).

^b $p < 0.05$ compared with corresponding data from wild type strain (one-way ANOVA with Bonferroni correction).

^c NT, not tested.

as a positive and negative modulator of the transcription of aerobic and hypoxic genes, respectively (14).

It was recognized only recently that Hmx1p possesses classical heme oxygenase activity (15), raising the possibility that in addition to regulating cellular heme and iron levels, Hmx1p may also share some of the additional activities of mammalian HO-1. Here, we show that Hmx1p indeed is induced in response to different stresses in addition to iron starvation, and that it protects yeast cells against oxidant challenge in a glutathione-dependent manner and via transcriptional regulation of genes encoding known enzymes involved in cellular antioxidant defense.

EXPERIMENTAL PROCEDURES

Yeast Strains and Growth Conditions—Supplemental Table S1 lists the *Saccharomyces cerevisiae* strains used in this study. The *HA-HMX1* wild-type strain, which expresses a triple copy of the hemagglutinin (HA) epitope at the N terminus, was constructed by PCR epitope tagging as described (16) using the plasmid pMPY-3 \times HA (a kind gift from Dr. C. C. Philpott, National Institutes of Health, Bethesda, MD) and the following primers: 5'-CAGCACACATACTCACTCACACATA-AAATAACCGCAAAAATAGGGACCAAACGCTGG-3' and 5'-TAGCTCCTCCATGTCAGTGTGTGAGTGTATGATT-GTATTGCTACTGTCCTTCTGTAGGGCGAATTGGG-3'. Integration of the HA epitope was confirmed by PCR and by Western blotting. Strains were grown in rich YEPD medium (2% w/v glucose, 2% w/v bacto-peptone, 1% yeast extract) or minimal synthetic-defined media (0.17% yeast nitrogen base without amino acids, 0.5% ammonium sulfate, 2% w/v glucose) supplemented with appropriate amino acids and bases: 2 mM L-leucine, 4 mM L-isoleucine, 1 mM L-valine, 0.3 mM L-histidine, 0.4 mM L-tryptophan, 1 mM L-lysine, 0.15 mM adenine, 0.2 mM uracil. Media were solidified by the addition of 2% (w/v) agar.

Western Blot Analysis—Cell extracts were subjected to electrophoresis under reducing conditions on 4–12% NuPAGE mini-gels (Invitrogen) and proteins blotted onto nitrocellulose membranes (Amersham Biosciences). Cytosolic and nuclear extracts were prepared as described (17). Blots were incubated with either mouse monoclonal anti-HA (to localize Hmx1p) (Sigma, 1:5,000 dilution), rat anti-tubulin (loading control) (Abcam, 1:5,000), mouse anti-Pgk1 (cytosol marker)

(Invitrogen, 1:5,000), mouse anti-Nop2 (nucleus marker) (Abcam, 1:5,000), mouse anti-Dpm1 (marker for ER and nuclear membrane-ER network) (Molecular Probes, 1:500) or rabbit anti-Kar2 antibody (ER marker) (Santa Cruz Biotechnology, 1:1,000), and bound antibody visualized by chemiluminescence (ECL, Amersham Biosciences) following incubation with sheep anti-mouse immunoglobulin-horseradish peroxidase conjugate (Amersham Biosciences, 1:5,000), sheep anti-rat immunoglobulin-horseradish peroxidase conjugate (Sigma, 1:5,000), or goat anti-rabbit immunoglobulin-horseradish peroxidase conjugate (Abcam, 1:5,000).

Sensitivity to Oxidants—Cells were grown to exponential phase ($A_{600\text{ nm}} = 1$) in synthetic medium at 30 °C and treated with H₂O₂, diamide, or menadione at the concentration and for the time indicated. Aliquots of cells were removed, diluted in fresh YEPD medium, plated in triplicate on YEPD plates, and the number of viable colonies counted after 3 days of culture.

Plasmids—A galactose-inducible multi-copy plasmid containing *HMX1* was constructed in JMB671, obtained as a generous gift from Dr. G. Perrone, (University of New South Wales, Sydney, Australia). The *HMX1-HA* coding sequence was amplified by PCR from the *HMX1-HA* tagged strain (Table 1) (*HMX1-HAF* 5'-TTCTTGTCTCGACCATGTATATACGAT-3' and *HMX1-HAR* 5'-ATTGTCTGAGTCAGACTCCTTTGG-3') and cloned into JMB671 using Sall and XhoI sites introduced by the 5' and 3' oligonucleotides (underlined). Galactose-inducible multi-copy plasmids containing *GPX1*, *GSH1*, *CTT1*, and *MXR1* were purchased from Open Biosystems (Open Biosystems, Huntsville, AL).

Microarray Hybridization and Data Analysis—Cells were grown in triplicate to exponential phase ($A_{600\text{ nm}} = 1$) in minimal SD medium. Cells were broken in Trizol reagent (Invitrogen) by three cycles of vigorous mixing in the presence of acid-washed glass beads (45 s) and placed on ice for 30 s. RNA was then extracted according to the manufacturer's instructions, and its quality determined by spectrophotometry (Nanodrop) and by Bioanalyser (Ramaciotti Centre for Gene Function Analysis, University of New South Wales, Australia). Preparation of cRNA, probes, and hybridization to whole yeast genome microarrays (YG-S98, Affymetrix) was performed at the Ramaciotti Centre. Affymetrix Yeast Genome

2.0 Arrays contain probe sets for *S. cerevisiae* and *Schizosaccharomyces pombe*. The latter probes were excluded from the analysis and normalization was performed using the robust multi-array average (RMA) (18, 19) algorithm implemented in BioConductor. For each individual *S. cerevisiae* gene (probe set) on the array, fold-change, moderated *t*-statistics and corresponding *p* value (20) were calculated. Candidate differentially expressed genes with a significant Bonferroni adjusted *p* value < 0.05 and fold-change > 2.0 (*hmx1* versus WT) were identified.

Relative mRNA levels of the differentially expressed antioxidant enzymes were determined by RT-PCR. Cells were prepared and RNA extracted as described above. cDNA was synthesized using the SuperScript III First-Strand Synthesis System for RT-PCR (Invitrogen) according to the manufacturer's instructions. The resulting cDNA was then probed for *GPX1*, *GSH1*, *CTT1*, *MXR1*, *GPX1*, *GPX2*, and *ACT1* by PCR, using the primers listed in supplemental Table S2. Resulting RT-PCR products were visualized by agarose gel electrophoresis and quantified using ImageJ (NIH).

Biochemical Analyses—Total glutathione was determined based on the reduction of oxidized glutathione (GSSG) by GSSG-reductase and NADPH (21). Cells were harvested at exponential growth phase, washed three times with ice-cold PBS, and resuspended in ice-cold 8 mM HCl/1.3% (w/v) 5-sulfosalicylic acid. Cells were then broken as described above, the resulting mixture clarified by centrifugation (10 min, 13,000 × *g*, 4 °C), and total glutathione determined in the resulting supernatant. Glutathione peroxidase activity was determined using *tert*-butyl hydroperoxide (Sigma) as substrate. Reactions were started by the addition of cell lysates and followed as the oxidation of NADPH coupled to GSSG reduction by glutathione reductase (22). Catalase activity was determined by the loss of added H₂O₂ (10 mM) in 50 mM K-phosphate buffer (pH 7.0) containing 0.5 mM EDTA after addition of cell extract (23). Blanks were run in the absence of H₂O₂ and activity calculated using $\epsilon_{240\text{ nm}} = 39.4\text{ M}^{-1}\text{ cm}^{-1}$. Methionine sulfoxide reductase activity was determined as described previously (24). Briefly, the reaction mixture contained 0.4 mM NADPH, 5 mM free Met-*R*-SO (Sigma), and 5 μg of thioredoxin and 0.5 μl of thioredoxin reductase (both from *Escherichia coli*, Sigma). The reaction was started by the addition of cell extract and allowed to take place for 15 min at 37 °C. Phosphate-buffered saline (200 μl) was then added and loss of NADPH determined immediately in a spectrophotometer using $\epsilon_{340\text{ nm}} = 6,220\text{ M}^{-1}\text{ cm}^{-1}$.

Immunocytochemistry and Confocal Microscopy—Cells were grown to exponential phase ($A_{600\text{ nm}} = 1$) in synthetic medium at 30 °C and treated for 6 h with H₂O₂ (4 mM). Cells were then washed and prepared for immunofluorescence microscopy as described (25), using anti-HA Alexa Fluor® 488-conjugated antibody (Molecular Probes) at 1:500 and the endoplasmic reticulum (ER) marker 3,3'-dihexyloxycarbocyanine iodide (DiOC₆ (3), Invitrogen) at a final concentration of 10 $\mu\text{g}/\text{ml}$.

Images were captured using a confocal laser microscope (Zeiss LSM Meta 510) with a 100× oil objective, 1.4-numerical-aperture at 12-bit resolution in each channel. Yeast

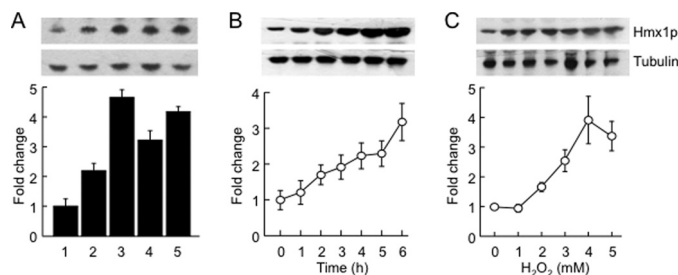


FIGURE 1. Hmx1p is induced in response to oxidative stress. A, cells grown to exponential phase in iron-replete (1) or iron-deprived (2, positive control) conditions, or in iron-replete condition for 6 h in the presence of 3 mM H₂O₂ (3), 3 mM diamide (4), or 10 mM menadione (5) were lysed, and the expression of Hmx1-HAP assessed by Western blotting relative to that of tubulin. B and C, cells grown to exponential phase in iron-replete conditions were treated with (B) 4 mM H₂O₂ for the indicated time, or (C) the indicated H₂O₂ concentration for 6 h. Following oxidant exposure, cells were lysed and the expression of Hmx1-HAP and tubulin assessed by Western blotting. A–C, upper panels show results typical of three separate experiments. The lower panels show quantitative data expressed as mean ± S.E. from the three separate experiments for each of the three conditions, with the respective density ratios of Hmx1p to tubulin determined using Quantity One, and with the respective ratio for (A) iron-replete non-stressed cells, (B) time 0, and (C) 0 H₂O₂ set at 1.

strains, without HA tag were used to control for background staining of the anti-HA Alexa conjugate. All captured images were converted to tagged image files, and Z-stacks collected at Z increments of 0.5 μm . Image processing three-dimensional analysis and z projection was performed using Image J software (NIH).

Statistical Analyses—Significant differences between treatments and controls were examined using the Wilcoxon-Mann-Whitney rank sum test. Where appropriate, data were analyzed by one- or two-way ANOVA with post-hoc Bonferroni test as indicated. Significance was accepted at *p* < 0.05.

RESULTS

Expression of Hmx1p Is Induced in Response to Different Oxidants—As HO-1 is induced in response to oxidant stress (4), we tested whether Hmx1p expression is induced similarly in yeast cells, using an HA-tagged *HMX1* strain and Western blotting with an anti-HA antibody (9). We noted modest expression of Hmx1p in control, unstressed cells (Fig. 1A, lane 1). Iron starvation increased Hmx1p expression (Fig. 1A, lane 2), confirming a finding reported previously by others (9). What is novel, however, is that Hmx1p was also induced when cells were exposed to H₂O₂, diamide (a membrane permeable, thiol-specific oxidant that reacts rapidly with reduced glutathione, GSH) and the redox-cycling drug menadione (that generates superoxide anion radicals) (Fig. 1A, lanes 3–5). Treatment of cells with H₂O₂ caused a time- (Fig. 1B) and oxidant concentration-dependent (Fig. 1C) increase in Hmx1p. Immunocytochemistry staining and confocal laser scanning microscopy confirmed low level of Hmx1p expression under standard, iron replete growth conditions (Fig. 2A, left panel arrows and boxed enlargements), and the increase in Hmx1p expression in cells exposed to iron starvation or H₂O₂ (Fig. 2, A and B). Yeast strains without HA tag yielded low background staining (Fig. 2C). The extent of H₂O₂-mediated increase in Hmx1p expression was comparable for N and C terminus HA-tagged *HMX1* strains (Fig. 2B). Whereas both

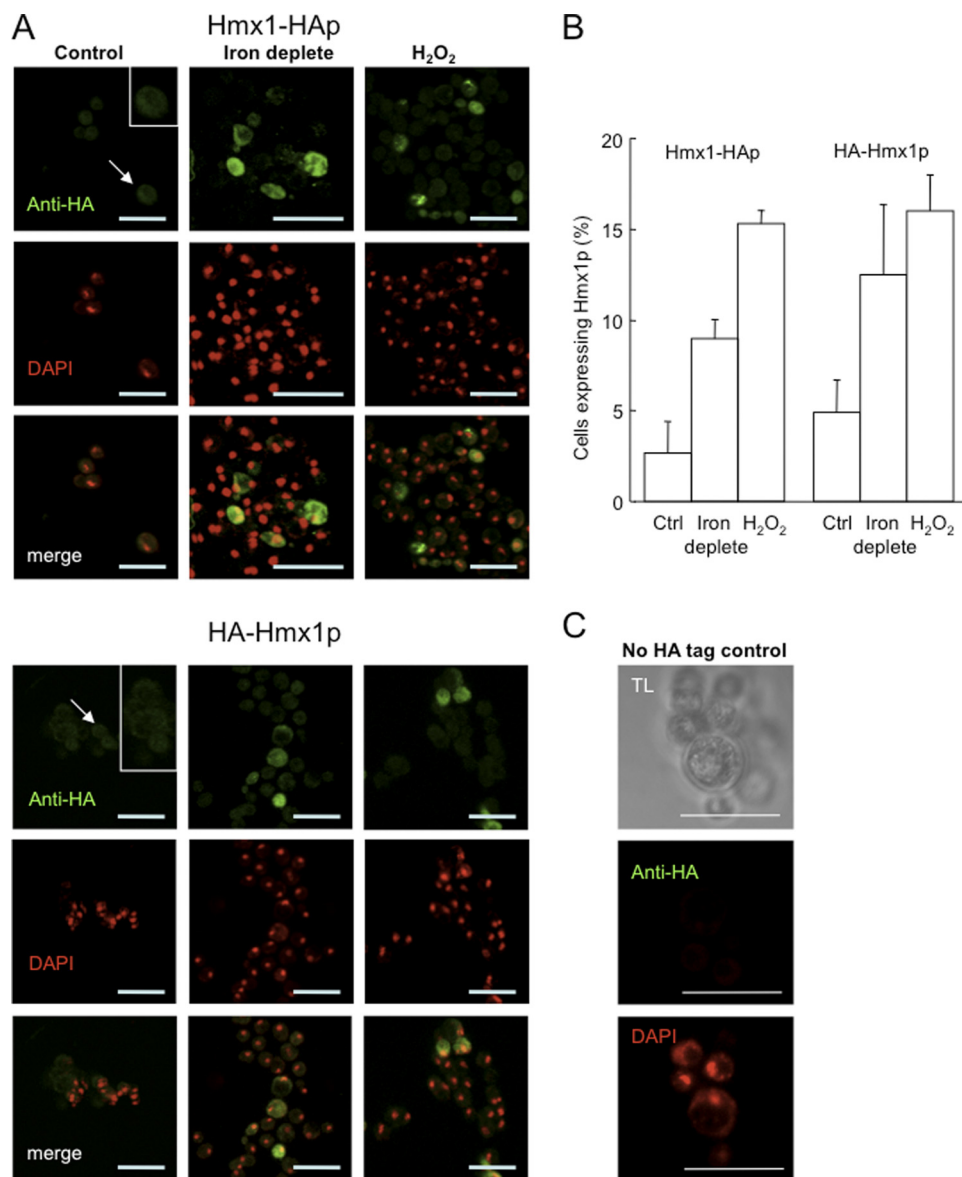


FIGURE 2. Heterogenous expression of Hmx1p in response to stress. *A*, confocal fluorescence images of yeast cells expressing Hmx1-HAp (top) or HA-Hmx1p (bottom) and stained with anti-HA Alexa 488 (green) and DAPI (red). Cells were grown at 30 °C in synthetic medium under iron replete (control, left panel) or iron deplete (middle panel) conditions, or treated for 6 h with 4 mM H₂O₂ (right panel) before being prepared for immunofluorescence microscopy. For each experimental setting several Z-stacks were collected at Z increments of 0.5 μm. Arrows denote control cells that display HA expression at low levels. Boxes show enlargements of selected cells. Scale bars, 10 μm. *B*, Hmx1 expression is increased upon iron deprivation or H₂O₂ treatment. Quantification of HA expression of cultures represented in *A*. Following three-dimensional image stack acquisition, the collected composite files of the z-stacks were analyzed and orthogonal planes were projected with the Image J software. Cells were counted that displayed notable staining with the anti-HA Alexa 488 antibody. Quantification of fluorescence images represents data (mean ± S.E.) from a single experiment with 3–8 independent z-stacks per treatment taken with identical settings. *C*, images of HA-tagged control cells. Parallel control cultures not expressing any HA-tagged constructs were prepared and microscopy performed with identical imaging settings as in *A*. Transmitted light (TL), anti-HA Alexa 488 (green), and DAPI (red) images are shown.

iron depletion and H₂O₂ increased Hmx1p expression visibly, the expression pattern was heterogenous, with very high expression in a subset of cells, but low to non-detectable expression in most cells (Fig. 2A). Hmx1p expression was also increased in response to other known inducers of HO-1, such as rapamycin and heat shock (not shown). The observed similarity between induction of HO-1 and Hmx1p in response to oxidative stress supports the contention that Hmx1p is part of the antioxidant defense in yeast cells.

HMX1 Affects Sensitivity to H₂O₂, Diamide, and Menadione—To test this possibility we compared the oxidant sensitivity of wild type and *hmx1* mutant cells using concen-

tration-response curves to H₂O₂, diamide, and menadione. At all concentrations tested, the *hmx1* mutant was more sensitive to the oxidants than the wild-type strain (Fig. 3A and supplemental Fig. S1A). Conversely, overexpression of *HMX1* increased the resistance of wild-type and *hmx1* mutant strains to H₂O₂ (Fig. 3B), diamide, and menadione (supplemental Fig. S1B). For the *hmx1* mutant strain, overexpression of *HMX1* restored the oxidant resistance to that of wild-type cells. Similarly, overexpression of *HMX1-HA* also fully rescued the oxidant sensitivity of the *hmx1*-null mutant (Fig. 3C and supplemental Fig. S1C), confirming that the HA-tagged Hmx1p used in our studies was functional. In addition, overexpression of

recombinant human HO-1 similarly rescued the oxidant sensitivity of the *hmx1* mutant (Fig. 3D). Together, these data indicate that Hmx1p is induced by, and offers protection

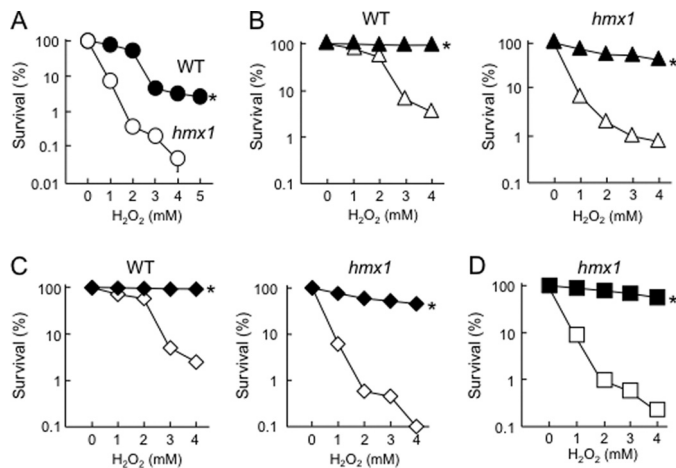


FIGURE 3. Loss of HMX1 renders the cell sensitive to H₂O₂, whereas overexpression of HMX1, HMX1-HA or human HO-1 rescues the *hmx1* sensitivity to oxidant challenge. A, wild type (●) and *hmx1* mutant strains (○) were grown to exponential phase in SD medium and treated for 1 h with H₂O₂ at the concentration indicated. Following treatment, cells were diluted and plated in triplicate onto YEPD medium to assess cell viability. B–D, wild type and *hmx1* mutant strains were transformed with a galactose-inducible multi-copy plasmid containing *HMX1* (B, triangles), *HMX1-HA* (C, diamonds), or the human HO-1 gene (D, squares). Cells were grown to exponential phase in raffinose- (non-induced, open symbols) or galactose-containing medium (induced, closed symbols) before treatment with H₂O₂. For human HO-1 overexpression (D), the *hmx1* mutant strain was used only. Survival is expressed as percentage of that seen with untreated control cells. Results show mean ± S.E. of a single experiment performed in triplicate, with standard error bars smaller than the symbols. *, *p* < 0.05 compared with wild type (A) or non-induced conditions (B–D) (two-ANOVA with Bonferroni correction).

against, oxidative stress, similar to the situation with HO-1 in mammalian cells.

The hmx1 Mutant Has Altered Expression of Cellular Antioxidant Enzymes—To determine if the transcriptional response of the *hmx1*-null mutant is altered compared with that of the wild-type strain, Affymetrix microarray analyses were carried out. Loss of *HMX1* significantly affected the transcriptome, with 265 open reading frames up-regulated (supplemental Table S3) and 215 down-regulated (supplemental Table S4) (Fig. 4A). Five gene ontologies were significantly over-represented in the up-regulated transcripts: response to stress, sulfur metabolic process, transcription factor activity, antioxidant activity, and transmembrane transporter activity. Two gene ontologies were significantly over-represented in the down-regulated transcripts: RNA processing and ribosome biogenesis.

We further investigated five transcripts encoding enzymes contributing to cellular antioxidant defense (Fig. 4B), the altered transcription of which was confirmed by RT-PCR (Fig. 5). Of these, *GSH1*, *GPX1*, *CTT1*, and *MXR1* were down-regulated, while *GPX2* was up-regulated. *GSH1* encodes γ -glutamylcysteine synthetase, which catalyzes the first step in the synthesis of GSH (26). It protects cells by scavenging oxidants and by acting as cofactor for several antioxidant enzymes (27). *GPX1* and *CTT1*, respectively, encode a glutathione peroxidase that acts on phospholipid hydroperoxides and other organic peroxides (22, 28), and a cytosolic catalase that forms part of a H₂O₂ detoxification system and is redundant with the glutathione system (29). *MXR1* encodes a peptide methionine sulfoxide reductase, which reduces methionine sulfoxide residues in proteins (30). *GPX2* encodes an atypical 2-Cys peroxiredoxin, responsible for the reduction of hydroperox-

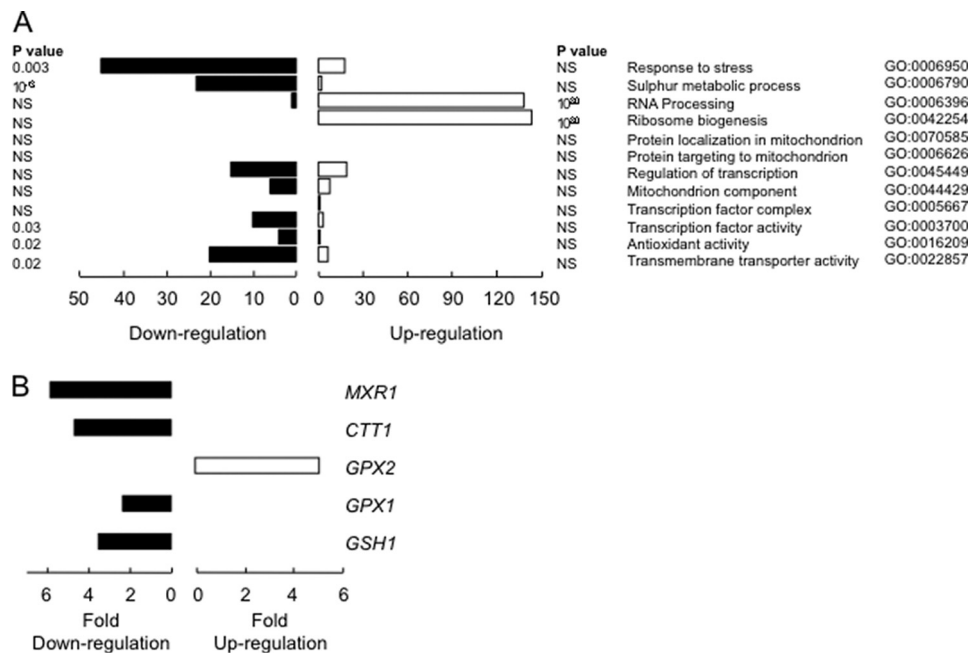


FIGURE 4. Functional categories of differentially expressed genes in *hmx1* deletion mutant compared with wild-type cells. Three separate cultures of each wild type and *hmx1* mutant strains were grown to exponential phase, their RNA extracted, and whole changes in the transcriptome analyzed using Affymetrix whole yeast genome microarrays (YG-S98), as described under "Experimental Procedures." A, genes up- or down-regulated in *hmx1* cells were sorted into groups according to the Gene Ontology Term Finder, provided by the *Saccharomyces* genome data base, with all data shown in supplemental Tables S3 and S4. B, antioxidant genes differentially expressed in *hmx1* cells.

Transcriptional Regulation by Heme Oxygenase-1

ides using thioredoxin rather than GSH as the preferred cofactor (31). This difference in cofactor preference may explain why *GPX1* and *GSH1* expression were down-regulated, while *GPX2* was up-regulated in the *hmx1* mutant. In addition to the five genes encoding known antioxidant enzymes, seven other transcripts with potential indirect participation in oxidative stress were also differentially expressed (supplemental Tables S3 and S4). The role of these genes was not investigated further.

Overexpression of Down-regulated Antioxidants Rescues Oxidant Sensitivity of *hmx1* Mutant—To define the mechanism of antioxidant protection by Hmx1p, each of the down-regulated antioxidant enzymes was overexpressed separately and the effect of this on rescue of *hmx1* oxidant sensitivity determined. Overexpressing either *GPX1* (Fig. 6A), *GSH1* (Fig. 6B), *CTT1* (Fig. 6C), or *MXR1* (Fig. 6D) increased resis-

tance of wild-type cells to diamide, H_2O_2 , and menadione. More importantly, overexpression of any of these genes also increased the resistance of the *hmx1* mutant to each of the three oxidants tested (Fig. 6, A–D). The extent of this increased resistance was less than that seen in the corresponding wild-type cells, indicating that each of the four known antioxidant enzymes alone partially rescued the oxidant sensitivity of the *hmx1* mutant strain. In contrast, simultaneous overexpression of all four transcripts encoding the antioxidant genes in the *hmx1* mutant (supplemental Fig. S2) completely restored its oxidant resistance to that of wild-type cells at all concentrations of H_2O_2 tested (Fig. 7).

HMX1 Relates to Cellular Antioxidant Activities—Consistent with the observed oxidant sensitivity, total glutathione concentration in the *hmx1* mutant was only ~20% of the wild-type strain value, and overexpression of *HMX1* in the *hmx1* mutant increased total glutathione to above wild-type levels (Table 1). Similarly, in the *hmx1* mutant, catalase and glutathione peroxidase activities were decreased compared with wild-type cells, and overexpression of *HMX1* increased the activity of both enzymes to above the corresponding wild-type values (Table 1). The activity of methionine sulfoxide reductase was below the limit of detection in all strains, except wild-type cells overexpressing *MXR1*. Together, these data show that the extent of *HMX1* expression relates to the cellular activities of the differentially expressed antioxidant enzymes identified in the microarray experiments.

We next examined whether in *hmx1* cells overexpression of each of the *HMX1* related antioxidant enzymes affected the activities of the other down-regulated antioxidants. As shown in Fig. 8, overexpression of *GSH1* increased both the content of total glutathione and glutathione peroxidase activity. Also, overexpression of *GPX1*, but not *CTT1* or *MXR1*, increased glutathione peroxidase activity (Fig. 8A). In the case of catalase, only overexpression of *CTT1* increased the activity of this enzyme (Fig. 8B), while overexpression of *GSH1* increased the levels of total glutathione (Fig. 8C). These results

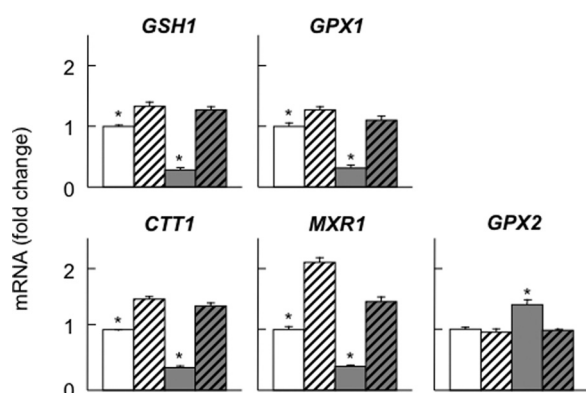


FIGURE 5. Deletion of *HMX1* or overexpression of *HMX1* affects the expression of antioxidant genes. Wild type (empty bars) and *hmx1* mutant strains (gray bars) without (no stripes) and with overexpression of the multi-copy plasmid containing *HMX1* (striped) were grown to exponential phase, the RNA extracted, and cDNA generated. The resulting cDNA was then probed for *GSH1*, *GPX1*, *CTT1*, *MXR1*, *GPX2*, and *ACT1* as described under "Experimental Procedures," and antioxidant gene expression shown relative to that of *ACT1*. Results represent mean \pm S.E. of three separate experiments. *, $p < 0.05$ compared with the corresponding *HMX1* overexpressing strain (one-way ANOVA with Bonferroni correction).

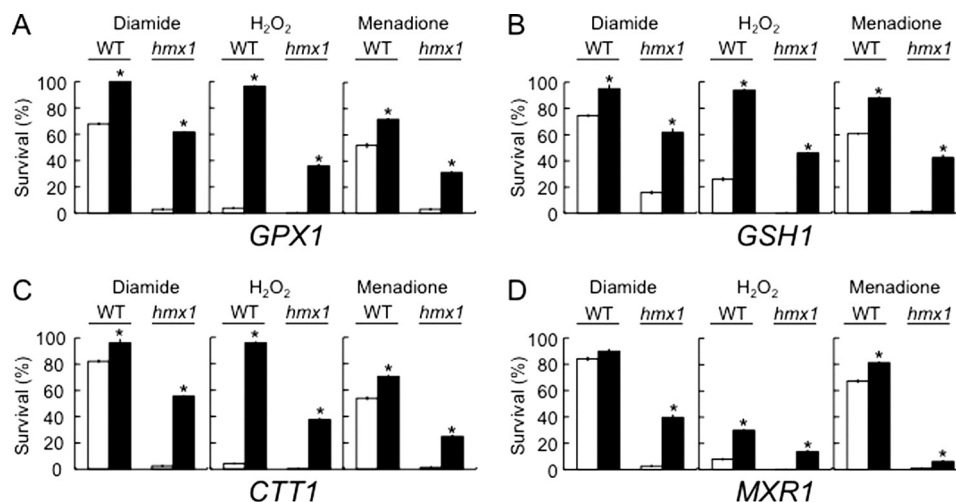


FIGURE 6. Overexpression of *GPX1*, *CTT1*, *GSH1*, or *MXR1* rescues oxidant sensitivity of *hmx1* deletion mutant. Wild type and *hmx1* mutant strains were transformed with a galactose-inducible multi-copy plasmid containing *GPX1* (A), *GSH1* (B), *CTT1* (C), or *MXR1* (D). Cells were grown to exponential phase in raffinose- (non-induced, open bars) or galactose-containing medium (induced, closed bars) and treated for 1 h with 4 mM diamide, 4 mM H_2O_2 , or 15 mM menadione. Survival is expressed as percentage of that seen with control cells. Results shown are mean \pm S.E. of a single experiment performed in triplicate. *, $p < 0.05$ compared with the corresponding non-induced strain (one-way ANOVA with Bonferroni correction).

indicate that the differentially expressed antioxidant genes, at least in part, acted independently from each other.

The fact that overexpression of all four transcripts encoding antioxidant genes was required to completely restore the oxidant resistance of the *hmx1* mutant (Fig. 7), suggested that the products of the reaction catalyzed by Hmx1p themselves

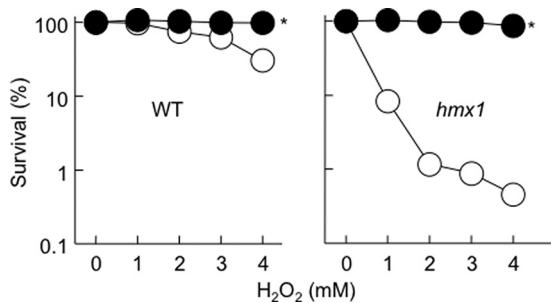


FIGURE 7. Simultaneous overexpression of GPX1, CTT1, GSH1, and MXR1 completely rescues oxidant sensitivity of *hmx1* deletion mutant. Wild type and *hmx1* mutant strains were transformed with 4 galactose-inducible multi-copy plasmids containing *GSH1*, *GPX1*, *CTT1*, and *MXR1*. Cells were grown to exponential phase in raffinose- (○) or galactose-containing medium (●) and treated for 1 h with H₂O₂ at the indicated concentration. Survival is expressed as percentage of that seen with control cells. Results shown are mean ± S.E. of a single experiment performed in triplicate, with standard error bars smaller than the symbols. *, $p < 0.05$ compared with the corresponding non-induced strain (two-way ANOVA with Bonferroni correction). There is no significant difference between wild type and *hmx1* mutant strains with all four antioxidant genes induced.

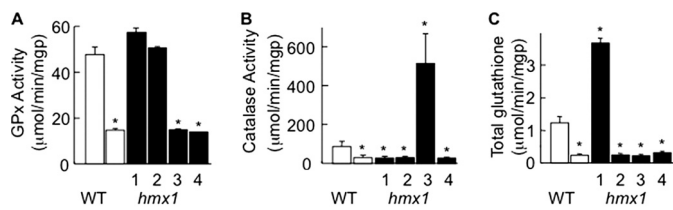


FIGURE 8. Altering the levels of antioxidants alters the activity of some but not all antioxidants. *hmx1* mutant strains were transformed with a galactose-inducible multi-copy plasmid containing *GSH1* (1), *GPX1* (2), *CTT1* (3), or *MXR1* (4). Cells were grown to exponential phase in raffinose- (non-induced, open bars) or galactose-containing medium (induced, closed bars) before the activity of (A) glutathione peroxidase or (B) catalase, and (C) total glutathione was determined as described under "Experimental Procedures." Results shown represent mean ± S.E. of three separate experiments. *, $p < 0.05$ compared with the corresponding wild-type strain (one-way ANOVA with Bonferroni correction). There were no differences between non-induced *hmx1* mutant and (A) the *hmx1* mutant with *CTT1* or *MXR1* induced, (B) *GSH1*, *GPX1*, or *MXR1* induced, and (C) *GPX1*, *CTT1*, or *MXR1* induced.

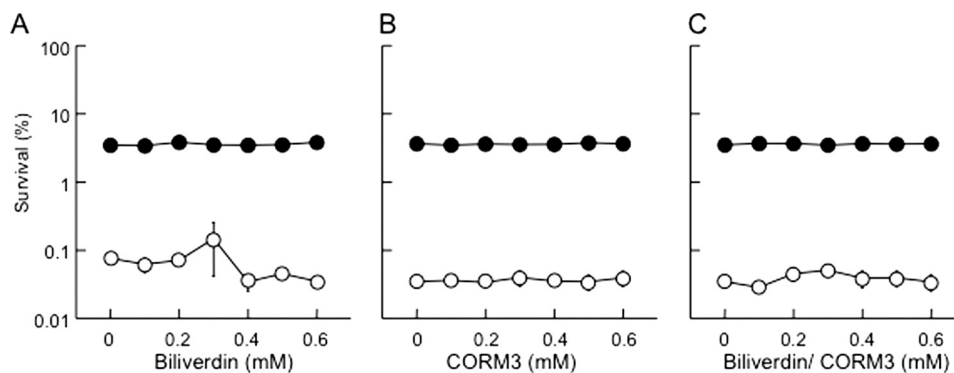


FIGURE 9. Addition of biliverdin or CORM3 fails to rescue *hmx1* oxidant sensitivity. Wild type (●) and *hmx1* (○) mutant strains were grown to exponential phase in SD medium and treated with 4 mM H₂O₂ for 1 h in the absence and presence of the indicated concentration of biliverdin (A), CORM3 (B) or both (C). Following treatment, cells were diluted and plated in triplicate onto YEPD medium to assess cell viability. Results shown represent mean ± S.E. of three separate experiments. Where S.E. bars cannot be seen, they are smaller than the symbol size.

did not provide substantial oxidant protection. Consistent with this interpretation, addition of biliverdin and the CO-releasing molecule CORM3, singly or together, failed to offer the *hmx1*-null mutant protection against 4 mM H₂O₂ (Fig. 9). Similar results were observed when cells were exposed to a lower H₂O₂ concentration (supplemental Fig. S3).

Dennerly and co-workers (32) recently reported HO-1 to localize to the nucleus of heme-treated mammalian cells and to activate transcription factors important in oxidative stress. In yeast, the nuclear and ER membranes are continuous (33), making it difficult to discriminate perinuclear from nuclear localization. We therefore use the term (peri)nuclear hereafter to refer to perinuclear or nuclear localization. We observed (peri)nuclear localization of Hmx1p in cells exposed to 4 mM H₂O₂ for 6 h, as assessed by microscopy and biochemical analyses (Fig. 10). Similar results were observed with cells stressed with H₂O₂ for 1 h (supplemental Fig. S4), indicating that (peri)nuclear localization of Hmx1p occurred even after short periods of oxidant stress. In contrast, (peri)nuclear Hmx1p was not detected in cells in the absence of H₂O₂. Following oxidant treatment, (peri)nuclear expression of Hmx1p was observed in only a small subset of cells (Fig. 10, A and B), with Hmx1p expressed more commonly in ER regions associated with membranes other than the nuclear membrane (supplemental Fig. S5). As in stressed mammalian cells nuclear localization has been reported to be preceded by calpain-mediated cleavage of the HO-1 C terminus (32), we compared the extent of (peri)nuclear localization of Hmx1p in N versus C terminus HA-tagged *HMX1* strains exposed to H₂O₂. We observed (peri)nuclear localization with both strains of yeast as assessed by confocal fluorescence microscopy (Fig. 10A) and biochemical analysis (Fig. 10C and supplemental Fig. S4). However, the extent was greater for N terminus than C terminus HA-tagged Hmx1p (Fig. 10, B and D and supplemental Fig. S4). As expected from the close physical association of nuclear and ER membranes, the nuclear fraction contained ER markers (Dpm1 and Kar2, Fig. 10C), disallowing unambiguous localization of Hmx1p to the nucleus.

DISCUSSION

The ability of cells to respond to changes in environmental conditions, such as nutrient availability, determines their sur-

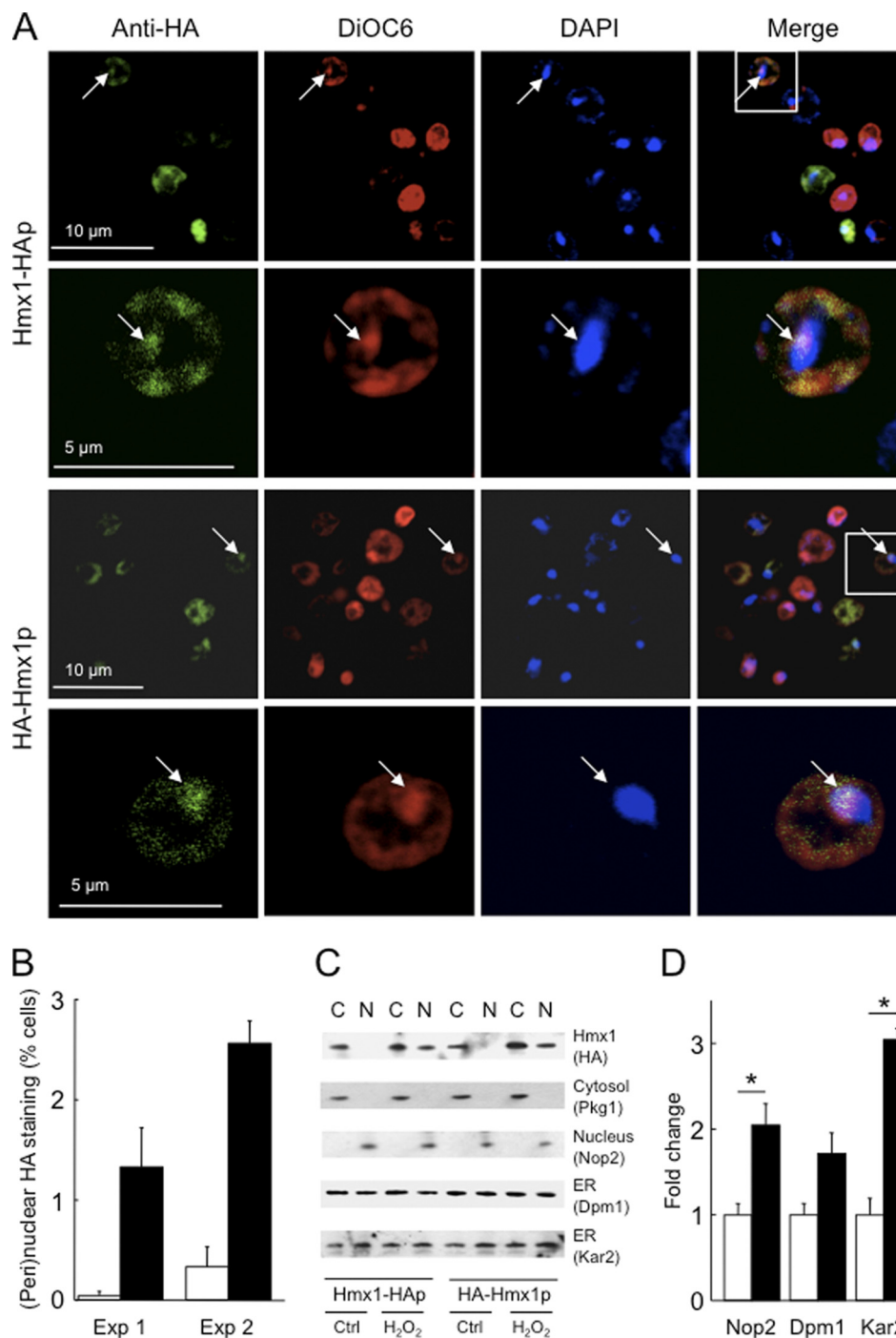


FIGURE 10. Heme oxygenase-1 translocates to the (peri)nuclear region in response to H₂O₂. *A*, confocal microscopy images of HA-tagged Hmx1p cells treated with 4 mM H₂O₂ for 6 h and then stained as described under "Experimental Procedures." Arrows denote areas (white) that show staining with all three markers, DAPI (blue), anti-HA (green), and ER marker DiOC6(3) (red), indicating (peri)nuclear localization of Hmx1p. Scale bars 10 or 5 μm, as indicated. *B*, quantification of the experiments shown in *A*. The extent of (peri)nuclear localization of Hmx1-HAp (open bars) and HA-Hmx1p (closed bars) in H₂O₂-treated cells was compared by counting cells that displayed distinctive (peri)nuclear staining, as assessed by acquisition and analysis of z-stacks taken of >1,000 cells for each of two separate experiments. *C*, cells were treated as in *A*, followed by cell fractionation into cytosolic (C) and nuclear fraction (N), and Western blotting using antibodies directed against HA (Hmx1p), Pkg1 (cytosol), Nop2 (nucleus), Dpm1p (ER), and Kar2 (ER). The results shown are representative of three separate experiments. *D*, quantification of the data obtained in *C*. The extent of (peri)nuclear/ER-localized Hmx1-HAp (open bars) and HA-Hmx1p (closed bars) in cells treated with H₂O₂ (4 mM, 6 h) was assessed by determining the respective density ratios of Hmx1p to either Nop2, Dpm1, or Kar2 from three separate experiments using ImageJ, with the value for the respective ratio for Hmx1-HAp set at 1. *, *p* < 0.05 compared with corresponding Hmx1-HAp (Wilcoxon Rank Sum Test).

vival. Until now, Hmx1p, the yeast homolog of HO-1, was believed to be involved only in the cellular response to iron limitation (9). Here we provide evidence that an additional role of Hmx1p is in the cellular response to and protection

against oxidative stress. Our studies, for the first time, show that this antioxidant activity of heme oxygenase is dependent on the up-regulation of several genes encoding known antioxidant enzymes.

Several lines of evidence support the conclusion that Hmx1p affords cellular antioxidant protection, and that this is via the transcriptional regulation of known antioxidant genes rather than its oxygenase activity. First, the expression of Hmx1p, like that of HO-1, is induced in cells exposed to different oxidants. Secondly, deletion of *HMX1* renders cells more sensitive to oxidant challenge while overexpression of *HMX1*, like human HO-1, restores oxidant resistance of the *hmx1*-null mutant to that of wild-type cells. Thirdly, microarray analyses revealed *GSH1*, *GPX1*, *CTT1*, and *MXR1* that encode well-established antioxidant defense enzymes to be down-regulated in the *hmx1*-null mutant compared with wild-type cells. Fourthly, overexpression of each of the down-regulated antioxidant genes partially rescues oxidant sensitivity of the *hmx1*-null mutant, while overexpression of all four down-regulated antioxidant genes provides complete protection to the null mutant. Furthermore, the levels of *HMX1* transcript mirrored (at least in the case of total glutathione, catalase, and glutathione peroxidase) the antioxidant activities of the genes down-regulated in the *hmx1*-null mutant. Therefore, changes to cellular glutathione and GSH-related antioxidant activities are likely key mechanisms by which Hmx1p protects cells against oxidants. This interpretation is consistent with the fact that in human cells one general mechanism of HO-1 induction is via modulation of cellular glutathione status (34).

It is now well established that HO-1 protects mammals against oxidative stress. For example, mice deficient in HO-1 have increased susceptibility to oxidative stress (35), and their cells are less capable to withstand an oxidative challenge than the corresponding wild-type cells (36), while HO-1 overexpression increases cellular resistance to oxidants (37). However, the mechanism underlying the antioxidant protection provided by HO-1 is not well understood. Early studies ascribed the antioxidant action to the HO-1 ability to simultaneously decrease the concentrations of the pro-oxidant heme and increase the levels of the antioxidant bilirubin (38). Bilirubin is an efficient oxidant scavenger *in vitro* (39), and when added at micromolar concentrations both bilirubin and the HO-1 substrate heme protect cells against oxidants (40). However, there is little direct evidence that bilirubin produced from endogenous heme as a consequence of increased HO-1 activity acts as a cellular antioxidant (41), and the amounts and sources of cellular heme available for degradation by HO-1 remain unknown. Indeed, addition of the products of heme oxygenase, biliverdin, and CO, had no measurable effect on the sensitivity of the *hmx1*-null mutant to H₂O₂ challenge (Fig. 9). Together, our results indicate that the antioxidant protection afforded by the yeast homolog of HO-1 is via an adaptive response that involves the transcriptional control of antioxidant genes, rather than directly via its oxygenase activity (Fig. 11). Transcriptional regulation by Hmx1p was observed with millimolar concentrations of H₂O₂, raising the question of physiological relevance. However, extrapolating oxidant concentrations from yeast to mammalian cells is complicated because of several species differences, including the oxidant resistance of the cell wall compared with plasma membrane (42), and redundancies in H₂O₂ metabolism (29).

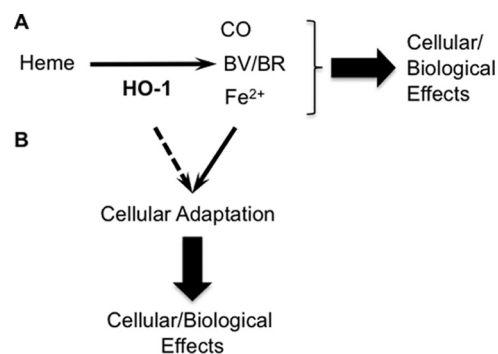


FIGURE 11. **Proposed new paradigm for cellular and biological functions of HO-1.** A, conventional view: cellular/biological effects of HO-1 result from its catalytic activity, *i.e.* the degradation of heme to CO, biliverdin/bilirubin (BV/BR) and Fe²⁺. B, proposed new paradigm: cellular/biological effects of HO-1 result from an adaptive response of cells to HO-1, independent (broken line) and/or dependent on HO-1 enzymatic activity (solid line).

In addition to catalyzing heme degradation and providing antioxidant protection, it is increasingly appreciated that HO-1 participates in the regulation of many biological processes, including inflammation, cell growth, vascular tone, and angiogenesis (4) that can translate into protection against various diseases (7, 43, 44). This raises the intriguing question of how HO-1 achieves these various activities. Using a global microarray analysis approach and yeast as a model, our studies revealed an unexpectedly large number of heme oxygenase-dependent, differentially expressed genes, the products of which are involved in several previously unrecognized processes, such as RNA processing, ribosome biogenesis, transcriptional regulation, and membrane transport (Fig. 4). In fact, of the differentially expressed genes, only a small number, corresponding to ~1%, relate to antioxidant defense. This indicates that at least in yeast, antioxidant protection may represent a relatively minor function of heme oxygenase, and that the enzyme likely participates in many presently unappreciated processes. For example, consistent with a regulatory role of HO-1 in the growth of mammalian cells, loss of *HMX1* increased the growth of yeast cells, and this was abrogated by overexpression of *HMX1* (not shown). This may relate to the differentially expressed genes involved in RNA processing and ribosome biogenesis (supplemental Tables S3 and S4). The down-regulation of transcripts encoding proteins involved in sulfur metabolism has been linked to increased oxidative stress (45) and hence may help explain the oxidant sensitivity of the *hmx1* mutant. Likewise, mammalian HO-1 has been reported to affect the activity of transcription factors (32), so that the down-regulation of transcription factors may help explain the inability of the *hmx1* mutant to mount an adequate response to oxidative stress.

Our microarray analyses also raise the question of how an ER protein can participate in transcriptional regulation. One possibility is that diffusible product(s) of heme oxygenase activity are involved. Indeed, a recent report suggested that in cardiomyocytes HO-1-derived CO regulates mitochondrial biogenesis via transcriptional regulation of nuclear respiratory factor-1 (46). Inconsistent with this notion, however, transfection of cells with a mutant HO-1 that lacks enzymatic activity still increased cellular resistance to H₂O₂ (37), and we ob-

served no protective effect of CO on the sensitivity of the *hmx1*-null mutant to H₂O₂ challenge (Fig. 9). We note however that our experimental design may not have adequately reflected local production of biliverdin/CO, perhaps close to or within the nucleus. An alternative explanation for the ability of HO-1 to regulate gene transcription has been provided by Dennery and co-workers (32) who reported that a C terminus truncated form of HO-1 migrates to the nucleus in response to hypoxia, hemin, and heme-hemopexin. We observed that in oxidant-stressed yeast cells, Hmx1p localized to the (peri)nuclear region where it could conceivably participate in the transcriptional regulation. We observed greater (peri)nuclear localization with N terminus than C terminus tagged Hmx1p, suggesting that translocation to the perinuclear region may precede cleavage. However, our results do not unambiguously establish nuclear localization or cleavage of Hmx1p. Indeed, integral ER proteins can enter the nucleus without a need for proteolytic cleavage (33). Clearly, additional studies are required to elucidate the mechanism by which Hmx1p affects transcriptional regulation.

In summary, our data show that in yeast the HO-1 homolog provides antioxidant protection to cells indirectly via the differential expression and activities of several known antioxidant enzymes. Our findings challenge the paradigm that the cellular/biological effects of HO-1 are explained solely by its enzymatic activity. Instead, they suggest that at least some of the HO-1 cellular/biological effects are the result of an adaptive response by the cells (Fig. 11). Clearly, *HMX1* regulates the expression of a large number of genes involved in numerous functions unrelated to heme oxygenase or antioxidant activities. Elucidating the relationship of heme oxygenase with these differentially expressed genes will likely unravel a multitude of novel functions of HO-1.

Acknowledgments—We thank Dr. Gabriel Perrone for the kind gift of plasmids, Dr. Anthony Cooper for anti-Dpml antibody, and Dr. Bernie Changsiri for help with the statistical analyses. We also thank Dr. Caroline Philpott for the kind gift of strains and for helpful comments on the manuscript.

REFERENCES

- Tenhunen, R., Marver, H. S., and Schmid, R. (1969) *J. Biol. Chem.* **244**, 6388–6394
- Cruse, I., and Maines, M. D. (1988) *J. Biol. Chem.* **263**, 3348–3353
- Maines, M. D., Trakshel, G. M., and Kutty, R. K. (1986) *J. Biol. Chem.* **261**, 411–419
- Ryter, S. W., Alam, J., and Choi, A. M. (2006) *Physiol. Rev.* **86**, 583–650
- Williams, S. E., Wootton, P., Mason, H. S., Bould, J., Iles, D. E., Riccardi, D., Peers, C., and Kemp, P. J. (2004) *Science* **306**, 2093–2097
- Yi, L., and Ragsdale, S. W. (2007) *J. Biol. Chem.* **282**, 21056–21067
- Stocker, R., and Perrella, M. A. (2006) *Circulation* **114**, 2178–2189
- Abraham, N. G., and Kappas, A. (2008) *Pharmacol. Rev.* **60**, 79–127
- Protchenko, O., and Philpott, C. C. (2003) *J. Biol. Chem.* **278**, 36582–36587
- Shakoury-Elizeh, M., Tiedeman, J., Rashford, J., Ferea, T., Demeter, J., Garcia, E., Rolfes, R., Brown, P. O., Botstein, D., and Philpott, C. C. (2004) *Mol. Biol. Cell* **15**, 1233–1243
- Yamaguchi-Iwai, Y., Dancis, A., and Klausner, R. D. (1995) *EMBO J.* **14**, 1231–1239
- Askwith, C., Eide, D., Van Ho, A., Bernard, P. S., Li, L., Davis-Kaplan, S., Sipe, D. M., and Kaplan, J. (1994) *Cell* **76**, 403–410
- Stearman, R., Yuan, D. S., Yamaguchi-Iwai, Y., Klausner, R. D., and Dancis, A. (1996) *Science* **271**, 1552–1557
- Kwast, K. E., Burke, P. V., and Poyton, R. O. (1998) *J. Exp. Biol.* **201**, 1177–1195
- Kim, D., Yukl, E., Moënné-Loccoz, P., and Montellano, P. R. (2006) *Biochemistry* **45**, 14772–14780
- Schneider, B. L., Seufert, W., Steiner, B., Yang, Q. H., and Futcher, A. B. (1995) *Yeast* **11**, 1265–1274
- Reeves, W. M., and Hahn, S. (2003) *Mol. Cell Biol.* **23**, 349–358
- Irizarry, R. A., Bolstad, B. M., Collin, F., Cope, L. M., Hobbs, B., and Speed, T. P. (2003) *Nucleic Acids Res.* **31**, e15
- Irizarry, R. A., Hobbs, B., Collin, F., Beazer-Barclay, Y. D., Antonellis, K. J., Scherf, U., and Speed, T. P. (2003) *Biostatistics* **4**, 249–264
- Smyth, G. K. (2004) *Stat. Appl. Genet. Mol. Biol.* **3**, Article3
- Chang, S. W., Lauterburg, B. H., and Voelkel, N. F. (1988) *J. Appl. Physiol.* **65**, 358–367
- Inoue, Y., Matsuda, T., Sugiyama, K., Izawa, S., and Kimura, A. (1999) *J. Biol. Chem.* **274**, 27002–27009
- Lushchak, V., Semchyshyn, H., Mandryk, S., and Lushchak, O. (2005) *Arch. Biochem. Biophys.* **441**, 35–40
- Le, D. T., Lee, B. C., Marino, S. M., Zhang, Y., Fomenko, D. E., Kaya, A., Hacıoglu, E., Kwak, G. H., Koc, A., Kim, H. Y., and Gladyshev, V. N. (2009) *J. Biol. Chem.* **284**, 4354–4364
- Philpott, C. C., and Protchenko, O. (2008) *Eukaryot. Cell* **7**, 20–27
- Ohtake, Y., and Yabuuchi, S. (1991) *Yeast* **7**, 953–961
- Meister, A., and Anderson, M. E. (1983) *Annu. Rev. Biochem.* **52**, 711–760
- Avery, A. M., and Avery, S. V. (2001) *J. Biol. Chem.* **276**, 33730–33735
- Grant, C. M., Perrone, G., and Dawes, I. W. (1998) *Biochem. Biophys. Res. Commun.* **253**, 893–898
- Moskovitz, J., Berlett, B. S., Poston, J. M., and Stadtman, E. R. (1997) *Proc. Natl. Acad. Sci. U.S.A.* **94**, 9585–9589
- Tanaka, T., Izawa, S., and Inoue, Y. (2005) *J. Biol. Chem.* **280**, 42078–42087
- Lin, Q., Weis, S., Yang, G., Weng, Y. H., Helston, R., Rish, K., Smith, A., Bordner, J., Polte, T., Gaunitz, F., and Dennery, P. A. (2007) *J. Biol. Chem.* **282**, 20621–20633
- King, M. C., Lusk, C. P., and Blobel, G. (2006) *Nature* **442**, 1003–1007
- Lautier, D., Luscher, P., and Tyrrell, R. M. (1992) *Carcinogenesis* **13**, 227–232
- Poss, K. D., and Tonegawa, S. (1997) *Proc. Natl. Acad. Sci. U.S.A.* **94**, 10919–10924
- Poss, K. D., and Tonegawa, S. (1997) *Proc. Natl. Acad. Sci. U.S.A.* **94**, 10925–10930
- Hori, R., Kashiba, M., Toma, T., Yachie, A., Goda, N., Makino, N., Soejima, A., Nagasawa, T., Nakabayashi, K., and Suematsu, M. (2002) *J. Biol. Chem.* **277**, 10712–10718
- Stocker, R. (1990) *Free Radic. Res. Commun.* **9**, 101–112
- Stocker, R., Yamamoto, Y., McDonagh, A. F., Glazer, A. N., and Ames, B. N. (1987) *Science* **235**, 1043–1046
- Clark, J. E., Foresti, R., Green, C. J., and Motterlini, R. (2000) *Biochem. J.* **348**, 615–619
- Stocker, R. (2004) *Antioxid. Redox. Signal* **6**, 841–849
- Sousa-Lopes, A., Antunes, F., Cyrne, L., and Marinho, H. S. (2004) *FEBS Lett.* **578**, 152–156
- Yachie, A., Niida, Y., Wada, T., Igarashi, N., Kaneda, H., Toma, T., Ohta, K., Kasahara, Y., and Koizumi, S. (1999) *J. Clin. Invest.* **103**, 129–135
- Deshane, J., Chen, S., Caballero, S., Grochot-Przeczek, A., Was, H., Li Calzi, S., Lach, R., Hock, T. D., Chen, B., Hill-Kapturczak, N., Siegal, G. P., Dulak, J., Jozkowicz, A., Grant, M. B., and Agarwal, A. (2007) *J. Exp. Med.* **204**, 605–618
- Wu, C. Y., Roje, S., Sandoval, F. J., Bird, A. J., Winge, D. R., and Eide, D. J. (2009) *J. Biol. Chem.* **284**, 27544–27556
- Piantadosi, C. A., Carraway, M. S., Babiker, A., and Suliman, H. B. (2008) *Circ. Res.* **103**, 1232–1240